Design of a Permanent-Magnet Synchronous Generator for a 2 MW Gearless Horizontal-Axis Wind Turbine According to its Capability Curve

A. Darijani*, A.Kiyoumarsi*, H.A.Lari*, B.Mirzaeian.Dehkordi*,S.Bekhrad*

Abstract: Permanent-Magnet Synchronous Generators (PMSGs) exhibit high efficiency and power density, and have already been employed in gearless wind turbines. In the gearless wind turbines, due to removal of the gearbox, the cogging torque is an important issue. Therefore, in this paper, at first design of a Permanent-Magnet Synchronous Generator for a 2MW gearless horizontal-axis wind turbine according to torque-speed and capability curves is presented. For estimation of cogging torque in PMSGs, an analytical method is used. Performance and accuracy of this method is compared with the results of Finite Element Method (FEM). With considering the effect of dominant design parameters, cogging torque is reduced considerably.

Keywords: Permanent-Magnet Synchronous Generator, Power Coefficient, Magnetic Voltage, Cogging Torque.

1 Introduction

Energy crisis and environmental pollution caused by fossil fuel, has led many countries to make effective use of wind energy for electric power generation. The horizontal axis wind turbines due to great heights from the ground have a good variant to generate electricity at high power levels [1].

Generators used in wind turbines are divided into two types of constant speed and variable speed. Until the late 1990s, most wind turbines were built for constant speed. The power level in these generators is below 1.5 MW and a multi-stage gearbox to maintain a constant speed is used. Nowadays most wind turbine manufacturers are building variable speed wind turbine for power levels from approximately 1.5 to 5 MW [2]. Recently, PMSGs due to high efficiency and power density have been greatly considered to produce power at different levels [3].

In wind turbines, in order to increase rotational speed of the shaft, gearboxes are used. But due to mechanical, repairing and noise problems it is removed and so called direct-drive generators are announced [4]. In this case, in order to compensate for the lack of speed by removing the gearbox, the number of poles in generator should be increased.

One of the disadvantages of the direct-driven generators is the cogging torque which is the main part of the torque pulsation. The cogging torque is the interaction between the Permanent-Magnets (PMs) and the stator slots [5]. Due to direct connection of the wind turbine and generator shaft, torque pulsation has a great concern and has direct impact on the efficient use of the wind power. Therefore less torque ripple developed by the system, reduces the mechanical stress and lowers the maintenance cost. The cogging torque calculation is discussed in many technical papers. In [6] an analytical method is used for this purpose with neglecting the motor's curvature. In [7 - 8] an analytical method is used to optimize small motors which have not a suitable prediction in large machines. Five different methods for calculating the cogging is comprised in [9].

In this paper, according to the speed-torque and capability curves, the area of operations to generate constant power for the generator is selected. The Generator's design is done in this interval, then using an analytical method the generator cogging torque is predicted and the results are compared with FEM. With considering the effect of design parameters, cogging torque is reduced considerably.

Iranian Journal of Electrical & Electronic Engineering, YYYY.
Paper first received DD MMM YYYY and in revised form DD MMM YYYY.
* The Authors are with the Department of Electrical Engineering, Faculty of Engineering, University of Isfahan, Isfahan, Iran.
E-mail: ahaddarijani@gmail.com,kiyoumarsi@eng.ui.ac.ir.
Corresponding Author: A. Kiyoumarsi.

2 Wind Turbine

In the wind turbine, power coefficient and Tip Speed Ratio (TSR) are two relevant definitions which describe the behavior of the wind turbine. The power coefficient (C_P), is defined as power output form the wind turbine to power contained in the wind and TSR is defined as follows [10]:

$$\lambda = \frac{\omega R}{V_\infty} \tag{1}$$

where R is the turbine radius, ω is rotational speed and V_∞ is wind speed.

The graph of the power coefficient against the TSR is a very important measure in characterizing the wind energy conversion. Fig. 1 illustrates the capability curves of the turbine for different pitch angles.

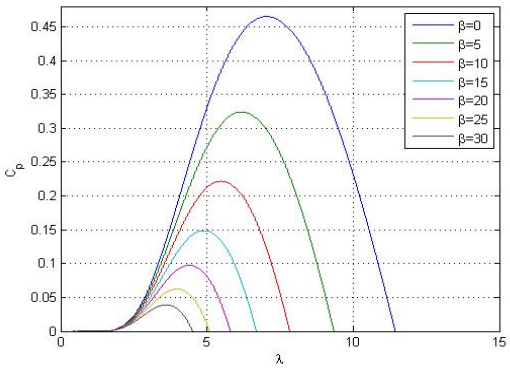

Fig. 1 Capability curve

The wind power is transmitted through the shaft to the generator and is converted into electrical power. Mechanical torque transmitted by the shaft of the wind turbine is expressed as [12]:

$$T = \frac{1}{2} C_P \pi \frac{R^5}{\lambda^3} \omega^2 \tag{2}$$

The main specifications of 2 MW wind turbine is showed in Table 1. According to Table 1 and Eq. (2), the Turbine's torque can be calculated.

Table 1 The main characteristics of the wind turbine

Parameter	Value
Rated Power (kW)	2050
Rotor Diameter (m)	92.5
Cut-in (m/s)	3
Cut-out (m/s)	25
Rotational Speed (rpm)	7.8-23 + 12.5%

The torque transmission equation in a turbine-generator system is considered as follows [12]:

$$T = T_L + J\frac{d}{dt}(\omega_m) + D\omega_m \tag{3}$$

where T_L is the generator torque, J is the inertia of the shaft of turbine, generator and the blades and D is the equivalent damping factor.

Generator design should take place based on the maximum power output of the turbine in steady-state operation. In this case, the variation of speed should be considered as zero.

In order to achieve the equilibrium in the system for the steady-state operation, the variations of generator's torque to speed should be greater than the variations of turbine's torque to speed. In other words the stability of system is satisfied when

$$\left(\frac{dT_L}{d\omega_m} - \frac{dT}{d\omega_m}\right) > 0 \tag{4}$$

where T_L is the generator's torque, T is the turbine's torque and ω_m is the mechanical rotational speed.

As it is understandable from the above equations, the power transmission can occur in an area of the torque curves that the slope of the turbine's torque curve is negative and the generator's torque curve is positive. In Fig. 2 the torque curves of generator and turbine are illustrated.

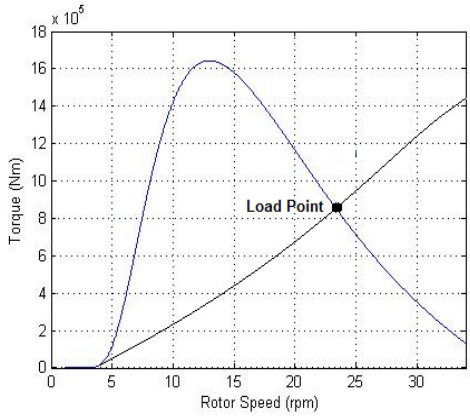

Fig 2. The turbine and generator's torque versus rotor speed curves

As can be seen from Fig. 2, The operational area for the transmission of power from the turbine to the generator is in speeds higher than the speed of maximum torque.

3 Design of the Generator

The Low-carbon steel and silicon-steel laminations are used in the rotor and stator of PMSG. The slot has semi-closed shape. The magnets are providing the air-gap flux density to generate power and are mounted on the exterior surface of the rotor. Between the two rare-earth permanent-magnets (NdFeB, SmCo), the NdFeB is preferred because it is cheaper and is already more available [12]. Therefore, NdFeB magnets are selected for the use in the PM generators. The primary parameters that affect a PM machine's dimensions are the air-gap

length and the magnet height. In [13], based on analytical and practical process, different methods for estimating the proper air-gap length are presented. These two parameters play a major role in determining the air-gap magnetic field, the air-gap flux density and the induced voltage in the machine.

3.1 Air-gap Flux Density

Air-gap flux density is determined according to saturation level of the stator. If the air-gap flux density is high enough to saturate the stator's core material, it will reduce the machine's performance. Therefor a balance must be established between magnetic circuit saturation and power absorption capability. For the considered generators, the flux density in the air-gap considered as 0.8 [T]. The fundamental component of the air-gap flux density is determined according to [14]:

$$B_{1\,peak} = \frac{4\sin\left(\alpha_{pm}\frac{\pi}{2}\right)}{\pi} B_{max} \tag{5}$$

where α_{pm} is the pole-arc to pole-pitch ratio and B_{max} is the maximum air-gap flux density.

3.2 Main Dimensions of the Generator

The first step to obtain the dimensions of the permanent-magnet surface-mounted generator is to choose appropriate tangential stress (σ-Ftan). The tangential stress is a factor that produces torque in these machines. The tangential stress depends on linear current density and flux density. The torque equation is expressed as [14]:

$$T = \sigma_{F\tan}\pi\frac{D_r^2}{2}l' \tag{6}$$

The diameter-to-length ratio in the generator is described as:

$$\frac{D_r}{l'} = \chi \tag{7}$$

where D_r is the rotor diameter and l' is the rotor equivalent length.

3.3 Stator and Rotor Yokes

Stator and rotor yokes provide a path for the flux to be circulated in the machine. The height of the stator and rotor yokes depends on the saturation level of the core. The efficiency of the machine can deteriorate by choosing the yoke too small; on the other hand the yoke cannot be selected over a specific size due to the machine's oversize. By selecting the maximum valid value for the flux density, the height of the stator and rotor yokes can be calculated as follows:

$$h_{yr} = \frac{\phi_m}{2k_{Fe}(l - n_v b_v)B_{yr}} \tag{8}$$

$$h_{yr} = \frac{\phi_m}{2k_{Fe}(l - n_v b_v)B_{yr}} \tag{9}$$

Where ϕ_m is magnetic flux, B_{yr} is rotor yoke flux density, B_{ys} is stator yoke flux density, b_v is width of the ventilation duct, n_v is number of the ventilation ducts and k_{fe} is the space factor for lamination.

3.4 Magnetic Voltage

With the passage of magnetic flux in different parts of machine, a voltage is created which is called magnetic voltage. The magnetic voltage in different part of the machine depends on the magnetic resistance (reluctance) of that part. The relationship of the magnetic voltage in magnetic circuits is as follows:

$$U_m = \oint_l Hdl \tag{10}$$

where H is the magnetic field and l is the path's length.

The air-gap has the highest magnetic voltage drop in the machine due to high magnetic resistance in the region. This is defined as follows:

$$U_{m\delta e} = \frac{B_{\max}}{\mu_0}.\delta_e \tag{10}$$

where μ_0 is the permeability of air and δ_e is the effective air-gap.

The product of the magnetic field strength of the stator teeth and its height results in teeth's magnetic voltage, which is defined as:

$$\hat{U_{md}} = H_d.h_d \tag{11}$$

Because of the nonlinearity between magnetic flux density and magnetic field strength, it results in nonlinear magnetic voltage in stator and rotor yoke, as for a coefficient c is used to determine the influence of the maximum flux density in yoke. The magnetic voltages are as follow:

$$U_{mys} = c_s H_{ys}\tau_{ys} \tag{12}$$

$$U_{myr} = c_r H_{yr}\tau_{yr} \tag{13}$$

In which H_y is field strengths corresponding to the highest flux density and τ_y is the lengths of the pole-pitch in the middle of the yoke.

3.5 Magnets Dimensions

The induced magnetic voltage in all parts of the machine is resulted from the flux of the magnets. In other words it is the magnet's flux that produces the magnetic voltage. An approximation to calculate this parameter is as:

$$U_{mtot} = H_c h_{PM} \tag{14}$$

with the expansion, the above relations, permanent-magnet height is calculated as follow:

$$h_{PM} = \frac{U_{m\delta e} + U_{mds} + \frac{U_{mys}}{2} + \frac{\pi c_r H_{ymaxr}.(D_r - h_{yr})}{4p}}{H_c - \frac{H_c}{B_r}.B_{PM} + \frac{\pi c_r H_{ymaxr}}{2p}} \tag{15}$$

3.6 Winding Factor

Generator's windings are distributed on the stator-inner surface to produce a sinusoidal voltage. Thus, the flux penetrating the winding does not intersect all windings simultaneously, and there is a certain time difference in the flux passing through the windings. This phenomenon in the induced voltage is defined by a coefficient which is called distribution factor. The Electromotive Force (EMF) in the machine depends on the number of winding turns in addition to the winding factor that is dependent to each harmonic and air-gap flux. The EMF is defined as:

$$E_{pm(n)} = \omega_s \phi_n k_{wn} N \tag{16}$$

where ω_s is the synchronous rotation speed, ϕ_n is the magnetic flux, k_{wn} is the winding factor and N is the number of conductors.

The winding factor consists of distribution factor, pitch factor and skewing factor. The relation of the winding factor is defined as follow [15]:

$$K_w(n) = \frac{2\sin(n.\frac{\pi}{2} w_{\tau p})\sin(\frac{n\pi}{2.m})\sin[v.(\frac{S_{sq}}{\tau_p}\frac{\pi}{2})]}{q\sin(n.\pi.\frac{p}{Q}).n(\frac{S_{sq}}{\tau_p}\frac{\pi}{2})} \tag{17}$$

where m is the number of phases, $w_{\tau p}$ is a constant coefficient equal to 0.83, S_{sq} is the pitch of pole-pair, q is the number of slots per pole per phase and τ_p is the pole-pitch.

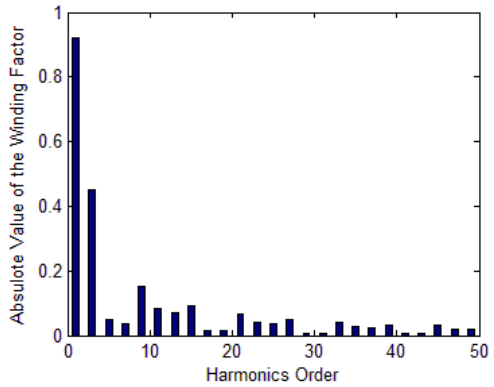

Fig. 3 Winding factor harmonics for q=1.6

The value for the winding factor harmonics for this generator is illustrated in Fig. 3.

3.7 Magnetizing Inductances

Due to similar values of permeability for air and permanent-magnet, the d-axis and q-axis inductances in PMSG have approximately the same values. The magnetizing inductance for a m-phase PMSM with distributed winding defines as:

$$L_{md} = L_{mq} = \frac{m}{2}.\frac{2}{\pi}\mu_0 l' \frac{1}{2.p}\frac{4}{\pi}\frac{\tau_p}{\delta_{ef}}(k_w(1)N)^2 \tag{18}$$

The d and q axis inductances are obtained from the leakage and magnetizing inductances. The leakage inductances in the electrical machines include the air-gap leakage inductance, slot leakage inductance, tooth tip leakage inductance and end-winding leakage inductance [14].

3.8 The Losses of the Generator

The losses in PMSM can be divided into several categories which are: stator Joules losses, mechanical losses, stray losses and iron losses. The iron losses are approximately proportional to the square of the yoke flux density and mass of the yoke. In addition, iron loss depends on the frequency of the generator. The maximum frequency is proportional to the rotational speed so by increasing the rotational speed, the iron loss will increase. An approximation to calculate the iron losses is as:

$$P_{Feys\ or\ Feyr} = k_{Fey} P_{15} (\frac{B_{ys\ or\ yr}}{1.5})^2 m_{ys\ or\ yr} (\frac{f}{50})^{\frac{3}{2}} \tag{19}$$

where f is the frequency, k_{Fey} is the correction factor, m_y is the mass of yokes, B_y is the yoke magnetic flux density and P_{15} is the loss correction factor.

3.9 The Torque-Load Angle Representation

The graph of the torque against the load angle is very important in characterizing the electrical machine. When the inductances and electromotive force are known, the torque relation with respect to load angle can be calculated. The torque equation against the load angle in the PMSMs is expressed as [16]:

$$T_e = \frac{m.p}{\omega_s^2}\left[\frac{E_{pm}.U}{L_{md} + L_{s\sigma}}\sin\delta\right] \tag{20}$$

where $L_{s\sigma}$ is the Leakage inductance and δ is the load angle.

Due to expected $L_d = L_q$, the maximum torque is achieved with load angle of 90°. Fig. 4 shows the torque curve plotted for this designed generator for a 288 slots and 60 poles combination.

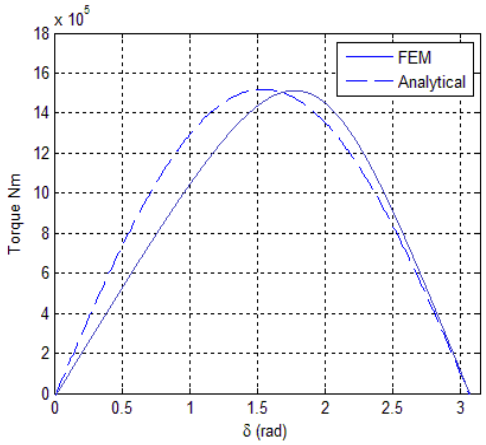

Fig. 4 Electrical torque versus angle load

In the Fig. 4 the dashed line is achieved from Eq. (20) results, and the continuous curve is obtained from the FEM results.

In Eq. (20) the d-axis and q-axis inductances are considered equally. But in the FEM, these values are closer to their actual values, thus there are a little difference with the values from Eq. (20). Due to this a slight difference can be seen in the curves.

4 FEM Analysis

The 2MW PMSG was designed and main characteristics and important dimensions are presented in Table 2 and 3.

Table 2 Electrical characteristics of the generator.

Name	Parameter	Value
Quadrature axis voltage (V)	v_{qs}^{r}	548.5
direct axis voltage (V)	v_{ds}^{r}	357.3
direct axis current (A)	I_{ds}	1465.32
Quadrature axis current (A)	I_{qs}	1225.21
Line voltage (V)	V_{LL}	660
Synchronous inductance (mH)	$L_d = L_q$	0.712
Rotor speed (rpm)	N	22

Table 3 Dimension characteristics of the generator

Name	Parameter	Value
Number of poles	$2.p$	60
Number of slots	Q	288
The Outer diameter of the stator(mm)	D_{se}	3890
The outer diameter of the rotor(mm)	D_r	3470
Effective length (mm)	l'	1293
Stator and rotor yoke height(mm)	h_{yr}	730
Magnet thickness(mm)	h_{PM}	25
Air-gap diameter(mm)	g	6

The finite element method was used to analysis the preliminary design in order to investigate the performance of the generator. Fig. 5 shows the generator prototype topology and magnetic flux lines in the full load condition. As can be seen in this situation, the maximum magnetic flux density occurs in the stator teeth. The phase-to-ground amplitude of the Back-EMF voltages of the designed generator are illustrated in Fig. 6.

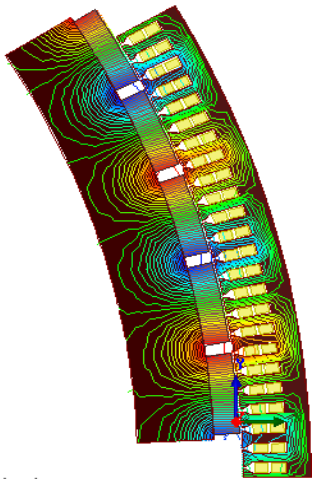

Fig. 5 Magnetic flux lines in full-load condition

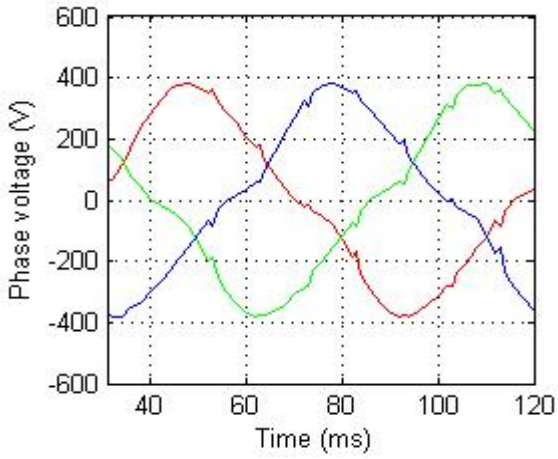

Fig. 6 Generator EMF phase voltages

The output torque of the generator for a period of constant wind speed in its optimum value is shown in Fig. 7. The electromagnetic torque in a PMSM consists of three parts. The main part is the interactive torque between the field of the magnets and of the stator windings. The other parts are ripple and the cogging torques. The reluctance torque is developed by the saliency of the rotor and the air-gap reluctance variations.

The cogging torque in PMSG is developed by the interaction between the magnetic field of the rotor magnets and the stator slots. The torque pulsation is defined as the sum of the ripple and the cogging torque.

in PMSGs a considerable portion of the torque ripple is caused by the cogging torque.

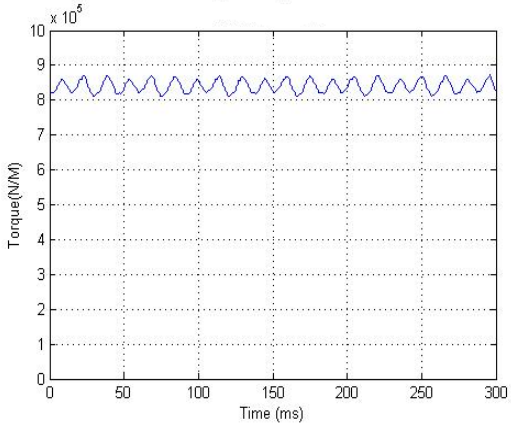

Fig. 7 Shaft torque versus time

5 Cogging Torque

In the wind turbines reducing the torque pulsations in the generator, results in an optimized usage of wind energy. In other words the less torque pulsation in the generator will result reducing the mechanical stress and higher efficiency of the system. The cogging torque is one of the inherent characteristics of PMSGs. In order to benefit more from wind energy, it is necessary to decrease this torque component as much as possible. The cogging torque is created due to variations in the energy in the air-gap when a magnet passes through the slot openings.

In this section an analytical method that is based on energy conversion in air-gap is used to calculate the cogging torque. This method is more accurate than any other analytical methods based on energy conversion [9]. In this method the following assumptions are considered:

- Neglecting the energy variation in the core.
- Considering the leakage flux in stator slots.
- Considering the inter-pole magnet leakage in PM model.
- Considering the curvature in PM and slot models.

By calculating the derivative of the air-gap field energy with respect to the rotational angle of the magnets, the cogging torque is obtained:

$$T_{cog}(a)=\frac{\partial W_{airgap}}{\partial a}=\frac{\partial}{\partial a}\left[\frac{1}{\mu_0}\int_v \frac{1}{\mu_0}G^2(\theta)B^2(\theta,a)dV\right] \tag{21}$$

where a is the position angle of the rotor, W_{airgap} is the magnetic energy in the air-gap, θ is the angle along the circumference, $G(\theta)$ is the air-gap relative permeance, and $B(\theta,a)$ is the air-gap flux density. The air-gap relative permeance is as follows [9]:

$$G(\theta)=\begin{cases}1 & \theta\in[-\pi/Q,-b_0/2]\cup[b_0/2,\pi/Q] \\ \dfrac{\frac{h_m}{\mu_r}+gC_\phi}{\frac{h_{pm}}{\mu_r}+[g-R_s+(R_s+\frac{\pi R_s}{2})\cos(\frac{b_0}{2}-|\theta|)]C_\phi} & \theta\in[-b_0/2,b_0/2]\end{cases} \tag{22}$$

where b_0 is the slot opening, μ_r is the magnet relative recoil permeability and C_ϕ is considered as [9]:

$$C_\phi=\frac{R_2-g-h_{pm}/2}{R_2-g/2} \tag{23}$$

The values for the $B_{a_{nNL}}$ and $G_{a_{nNL}}$ are as follows [9]:

$$G_{a_{nNL}}=Q/\pi\int_{-b_0/2}^{b_0/2}G(\theta)\cos(nN_L\theta)^2 \tag{24}$$

$$B_{a_{nNL}}=\frac{2p}{\pi}\int_0^{\pi/N_p}B(\theta)\cos(nN_L\theta)^2 d\theta \tag{25}$$

The air-gap flux density in an equivalent slot-less machine is as follows [9]:

$$B(\theta)=\sum_{i=1,3,5}^{\infty}\frac{4pB}{\mu}\sin(\frac{i\pi\alpha}{2})\frac{\left(\frac{R_m}{R_s}\right)^{\frac{iN}{2}+1}}{(\frac{ip}{2})-1}\left\{\frac{(\frac{ip}{2}-1)+2\left(\frac{R_s}{R_m}\right)^{\frac{ip}{2}+1}-\left(\frac{ip}{2}+1\right)\left(\frac{R_s}{R_m}\right)^{ip}}{\frac{\mu_r-1}{\mu_r}\left[1-\left(\frac{R_s}{R_s}\right)^{ip}\right]-\frac{\mu_r-1}{\mu_r}\left[(\frac{R_m}{R_s})^{ip}-(\frac{R_s}{R_m})^{ip}\right]}\right\}*\cos(\frac{ip}{2}\theta) \tag{26}$$

.

5.1 Comparing the Results of the Analytical Method and Finite Element Method

In this section the results for the air-gap flux density and cogging torque obtained by the analytical method and finite element method are compared. The results of both methods are shown in Fig. 8 and 9, respectively.

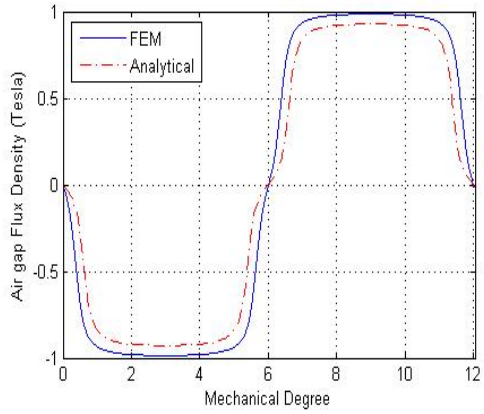

Fig. 8 Comparison of the air-gap flux density for the two methods.

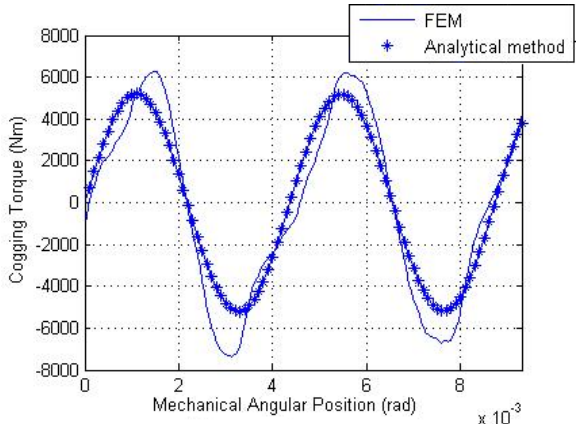

Fig. 9 Comparison of the cogging torque of two methods.

From Fig. 8, it can be seen that the amplitude of the air-gap flux density obtained from FEM is slightly greater than of the analytical method. But these curves are approximately the same.

Fig. 9, shows the difference for cogging torque between the results from the analytical method and the FEM. It can be seen that both curves are approximately close. The difference being seen in both Fig. 8 and 9 can be expressed by neglecting the energy variation in both magnets and core, ignoring the tangential component of the flux density and finally not percisely modeling the flux leakage and slot effects. The analytical method results an acceptable prediction for the cogging torque and can be used for sensebility analysis and optimization for cogging torque effective parameters.

5.2 Sensitivity Analysis of Effective Parameters on Cogging Torque

In this section the effects of peak cogging torque versus h_m, a_{pm}, g are investigated. In Fig. 10, the variation of the peak cogging torque with respects to a_{pm} is shown in part a. Part b is assigned to illustrate the peak cogging torque versus air-gap diameter and peak cogging torque versus magnet thickness is illustrated in part c.

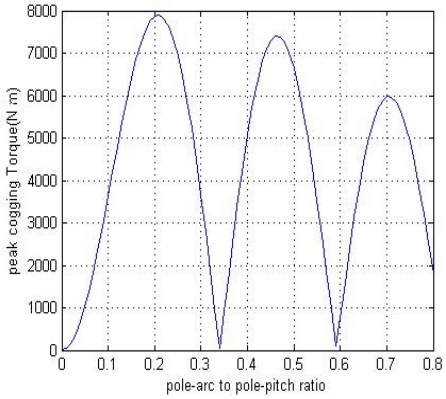

a: The peak cogging torque sensitivity to pole-arc to pole-pitch ratio

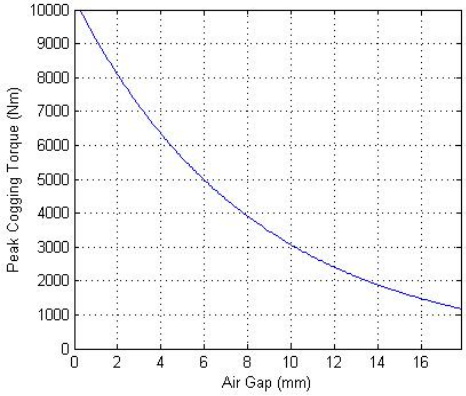

b: the peak cogging torque sensitivity to air-gap

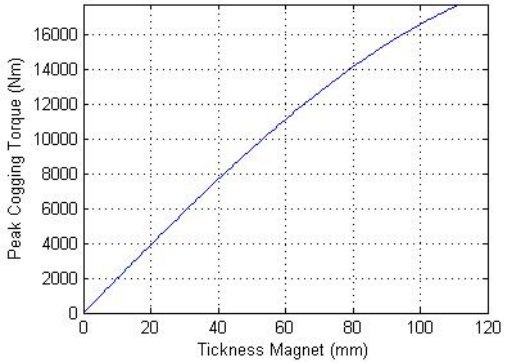

c: The peeak cogging torque sensitivity to thickness of the magnet

Fig. 10 The effect of some important parameters on the peak cogging torque

The magnetic flux density is amplified by increasing the magnets height which consequently increases the cogging torque. On the other hand by reducing the magnets height too much the flux density drops and arises problems like reducing the Back-EMF voltage amplitude. Thus, a trade off should be considered when choosing this parameter.

One of the outcomes in air-gap diameter reduction in the machine is the increase of total efficiency and vise versa. But it has drawbacks like cogging torque growth and mechanical limitations. Thus a trade off should be considered as well.

Due to the effect of mentioned parameters on the cogging torque a new set of parameters is choosed to redesign the generator. This parameters are shown in Table 4.

Table 4 Impropved parameter

Parameters	Initial	Improved
a_p (rad)	0.75	0.8
h_{pm} (mm)	30	25
g (mm)	5.5	6.5

As shown in Fig. 13, in the preliminary desing, the amplitude of cogging torque was nearly 6100 Nm and in the new design this value is reduced to 2000 Nm which is about 67% reduction.

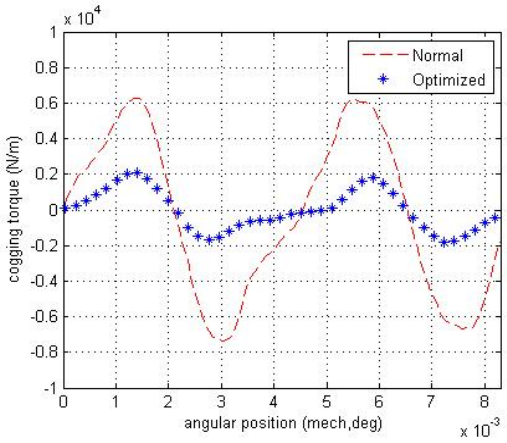

Fig. 11 Comparison the cogging torque, the result of changing of parameters in a proper manner

6 Conclusion

In this paper, the principle relations to describe the behavior of a wind turbine are discussed. Then, the torque-speed curves of the wind turbine and an exemplary curve for the generator were intercepted. The interception was in the practical power transmission intervals. An optimum loading point to design a 2 MW permanent-magnet synchronous generator is chosen. Throughout the stage of designing, some important parameters like main dimensions, magnet dimensions, winding factor and core losses are discussed. The torque versus load angle of the generator is obtained by two methods. An analytical method is used to calculate the cogging torque. The results are compared by that of the finite element method are approximately alike. Finally, the changes in some parameters are studied. The sensitivity of cogging torque to these parameters is illustrated. By considering the new values for some of the parameters, the cogging torque amplitude is also reduced.

References

[1] T. Burton, N. Jenkins, D. Sharpe, and E. Bossanyi, *Wind energy handbook*: John Wiley & Sons, 2011.

[2] H. Polinder, F. F. Van der Pijl, G. J. De Vilder, and P. J. Tavner, "*Comparison of direct-drive and geared generator concepts for wind turbines*," Energy conversion, IEEE transactions on, vol. 21, pp. 725-733, 2006.

[3] H. Haraguchi, S. Morimoto, and M. Sanada, "Suitable design of a PMSG for a large-scale wind power generator," *in Energy Conversion Congress and Exposition, ECCE 2009. IEEE*, pp. 2447-2452, 2009.

[4] B. Chalmers and E. Spooner, "An axial-flux permanent-magnet generator for a gearless wind energy system," *Energy Conversion, IEEE Transactions on*, vol. 14, pp. 251-257, 1999.

[5] N. Bianchi and S. Bolognani, "Design techniques for reducing the cogging torque in surface-mounted PM motors," *Industry Applications*, IEEE Transactions on, vol. 38, pp. 1259-1265, 2002.

[6] X. Wang, Y. Yang, and D. Fu, "*Study of cogging torque in surface-mounted permanent magnet motors with energy method*," *Journal of magnetism and magnetic materials*, vol. 267, pp. 80-85, 2003.

[7] T. Tudorache, L. Melcescu, and M. Popescu, "Methods for cogging torque reduction of directly driven PM wind generators," in *Optimization of Electrical and Electronic Equipment (OPTIM), 2010 12th International Conference on*, pp. 1161-1166, 2010.

[8] Y. Yang, X. Wang, R. Zhang, T. Ding, and R. Tang, "The optimization of pole arc coefficient to reduce cogging torque in surface-mounted permanent magnet motors," *Magnetics, IEEE Transactions on*, vol. 42, pp. 1135-1138, 2006.

[9] L. Zhu, S. Jiang, Z. Zhu, and C. Chan, "Comparison of alternate analytical models for predicting cogging torque in surface-mounted permanent magnet machines," in *Vehicle Power and Propulsion Conference, 2008. VPPC'08. IEEE*, pp. 1-6, 2008.

[10] S. N. Bhadra, D. Kastha, and S. Banerjee, Wind electrical systems: Oxford University Press, 2005.

[11] S. Eriksson, H. Bernhoff, and M. Leijon, "Evaluation of different turbine concepts for wind power," *Renewable and Sustainable Energy Reviews*, vol. 12, pp. 1419-1434, 2008.

[12] Mark Rippy, *An Overview Guide for the Selection of Lamination Materials*, Proto Laminations, Inc, 2004.

[13] T.A.Lipo, *Introduction to AC Machine Design*, University of Wisconsin Power Electronics Research Center, University of Wisconsin, Madison, vol.1, 1996.

[14] J.Pyrhonen, T.Jokinen, and V.Hrabovcova, *Design of Rotating Electrical Machin*John, Wiley & Sons, 2008.

[15] I. Boldea, *The induction machines design handbook*: CRC press, 2009.

[16] P. Bimbhra, Electrical Machinery Theory, Performance and Applications: Khanna, 1979.

Ahad Darijani was born in Kerman , Iran, in 1988. He received B.Sc. degree in Electronic Engineering from University of Lorestan, Khorramabad, Iran in 2010 and M.Sc. degree in Electrical Power Engineering from University of Isfahan, Isfahan, Iran in 2013. His research interests are on designing Interior permanent-magnet motors and generator, Linear Machines Optimization and Finite Element Method.

Arash Kiyoumarsi was born in Shahr-e-Kord, Iran, 1972. He received his B.Sc. (with honors) from Petruliom University of Technology (PUT), Iran, in electronics engineering in 1995 and M.Sc. from Isfahan University of Technology (IUT), Iran, in electrical power engineering in 1998. He received Ph.D. degree from the same university in electrical power engineering in 2004. His research interests have included application of finite element analysis in electromagnetics, interior permanent-magnet synchronous motor drives, shape design optimization and nonlinear control of electrical machines.

heidar ali lari was born in Sabzevar, Iran 1986. He received B.Sc. degree in electrical engineering from Birjand University, Birjand, Iran in 2011 and M.Sc. degree in electrical power engineering in University of Isfahan, Iran in 2013. Her research interest includes on application of finite element analysis and design of permanent magnet machines.

Behzad Mirzaeian Dehkordi was born in Shahrekord, Iran, in 1966. He received the B.Sc. degree in electronics engineering from Shiraz University, Shiraz, Iran, in 1985, and the M.Sc. and Ph.D. degrees in Electrical engineering from Isfahan University of Technology (IUT), Isfahan, Iran, in 1994 and 2000, respectively. From March to August 2008, he was a Visiting Professor with the Power Electronic Laboratory, Seoul National University (SNU), Seoul, Korea. His fields of interest include power electronics and drives, intelligent systems, and power quality problems.

Shahram Bekhrad received B.Sc. in Electrical Engineering from Shiraz University, Shiraz, Iran in 2010. He received M.Sc. degree in Electrical Power Engineering from University of Isfahan, Isfahan, Iran in 2013. His research interest is on electrical machine drives.